

Shizhong Wang · Xinyu Lu · Meilin Liu

Electrocatalytic properties of $\text{La}_{0.9}\text{Sr}_{0.1}\text{MnO}_3$ -based electrodes for oxygen reduction

Received: 12 March 2001 / Accepted: 15 August 2001 / Published online: 19 October 2001
© Springer-Verlag 2001

Abstract Electrochemical reduction of oxygen at the interface between a $\text{La}_{0.9}\text{Sr}_{0.1}\text{MnO}_3$ (LSM)-based electrode and an electrolyte, either yttria-stabilized-zirconia (YSZ) or $\text{La}_{0.8}\text{Sr}_{0.2}\text{Ga}_{0.9}\text{Mg}_{0.1}\text{O}_3$ (LSGM), has been investigated using DC polarization, impedance spectroscopy, and potential step methods at temperatures from 1053 to 1173 K. Results show that the mechanism of oxygen reduction at an LSM/electrolyte interface changes with the type of electrolyte. At an LSM/YSZ interface, the apparent cathodic charge transfer coefficient is about 1 at high temperatures, implying that the rate-determining step (r.d.s.) is the diffusion of partially reduced oxygen species, while at an LSM/LSGM interface the cathodic charge transfer coefficient is about 0.5, implying that the r.d.s. is the donation of electrons to atomic oxygen. The relaxation behavior of the LSM/electrolyte interfaces displays an even more dramatic dependence on the type of electrolyte. Under cathodic polarization, the current passing through an LSM/YSZ interface increases with time whereas that through an LSM/LSGM interface decreases with time, further confirming that it is the triple phase boundaries (TPBs), rather than the surface of the LSM or the LSM/gas interface, that dominate the electrode kinetics when LSM is used as an electrode.

Keywords Oxygen reduction · Lanthanum strontium manganite electrode · Electrode polarization · Impedance spectroscopy · Solid oxide fuel cells

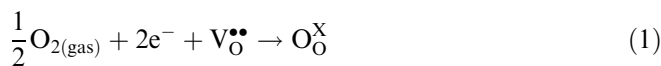
Introduction

Strontium-doped lanthanum manganite (LSM) has been widely used as a cathode material for high-temperature

solid oxide fuel cells (SOFCs) based on yttria-stabilized zirconia (YSZ), owing to its high catalytic activity for oxygen reduction, high electronic conductivity, and good chemical and thermal compatibility with YSZ. However, the catalytic activity of LSM for oxygen reduction at intermediate and low temperatures needs to be further investigated [1]. For low-temperature SOFCs, the YSZ electrolyte must be sufficiently thin (a few microns) to minimize ohmic losses and the long-term stability and durability of thin-film YSZ are yet to be demonstrated. LaGaO_3 -based electrolytes, such as $\text{La}_{0.9}\text{Sr}_{0.1}\text{Ga}_{0.9}\text{Mg}_{0.1}\text{O}_3$ (LSGM), exhibit much higher oxygen ion conductivity than YSZ at intermediate and low temperatures with adequate stability [1, 2, 3, 4]. It is also reported [1] that LSM electrodes supported on LSGM have a high activity for oxygen reduction at relatively low temperatures. LSGM has a good potential to be a viable electrolyte material for intermediate- and low-temperature SOFCs.

While LSM has high electronic conductivity, it is a poor mixed ionic and electronic conductor (MIEC) because of its relatively low ionic conductivity. Oxygen reduction takes place mainly at the triple phase boundary (TPB) rather than the LSM/gas interface when LSM is used as an electrode, especially at low overpotentials. When the cathodic overpotential is sufficiently high, the activity of an LSM electrode supported on YSZ increases dramatically; this was reportedly due to the extension of the active area from the TPB to the LSM/gas interface [5, 6, 7, 8, 9]. However, it is difficult to quantify the exact contribution of the LSM/gas surface.

The overall reaction for oxygen reduction at an LSM electrode can be expressed as:



where $\text{V}_{\text{O}}^{\bullet\bullet}$ and $\text{O}_{\text{O}}^{\times}$ represent an oxygen vacancy and an oxygen ion at a regular oxygen site, respectively. Phenomenologically, the relationship between the current passing through the interface, i , and the overpotential across the interface, η , can be described by the Butler-Volmer equation [10]:

S. Wang · X. Lu · M. Liu (✉)
School of Materials Science and Engineering,
Georgia Institute of Technology, Atlanta, GA 30332, USA
E-mail: meilin.liu@mse.gatech.edu
Tel.: +1-404-8946114
Fax: +1-404-8949140

$$i = i_0[\exp(\alpha_a F\eta/RT) - \exp(-\alpha_c F\eta/RT)] \quad (2)$$

where i_0 is the exchange current density, F is Faraday's constant, R is the universal gas constant, T is the absolute temperature, and α_a and α_c are the anodic and cathodic charge transfer coefficients, which are related to the number of electrons evolved in the overall reaction, n , and the number of times the rate-determining step (r.d.s.) occurs for one act of overall reaction, ν , as follows:

$$\alpha_a + \alpha_c = n/\nu \quad (3)$$

When the overpotential is sufficiently small, i.e., $|\eta| \ll (RT/F)$, Eq. 2 simplifies to:

$$i = i_0(\alpha_c + \alpha_a) \left(\frac{F\eta}{RT} \right) \quad (4)$$

Thus, the interfacial polarization resistance under this condition can be approximated by:

$$R_p = \left(\frac{\partial \eta}{\partial i} \right) = \left(\frac{RT}{F} \right) \left(\frac{1}{\alpha_a + \alpha_c} \right) \left(\frac{1}{i_0} \right) \quad (5)$$

and the exchange current density is given by:

$$i_0 = \left(\frac{RT}{F} \right) \left(\frac{1}{\alpha_a + \alpha_c} \right) \left(\frac{1}{R_p} \right) = \left(\frac{T}{R_p} \right) \left(\frac{R}{F(\alpha_a + \alpha_c)} \right) \quad (6)$$

When the cathodic overpotential is sufficiently high ($-\eta \gg RT/F$), Eq. 2 simplifies to:

$$i = -i_0 \exp(-\alpha_c F\eta/RT) \quad (7)$$

and the cathodic charge transfer coefficient can be determined from:

$$\alpha_c = \left(\frac{RT}{F} \right) \left(-\frac{1}{\eta} \right) \ln \left| \left(-\frac{i}{i_0} \right) \right| \quad (8)$$

Various models have been proposed to describe the mechanism for oxygen reduction at an LSM electrode. Listed in Table 1 are the charge transfer coefficients of a model proposed by Bouwmeester [5, 11, 12]. Under certain conditions, the r.d.s. for oxygen reduction could be deduced from the values of the charge transfer coefficients.

While the use of Butler-Volmer equation is effective in determining the mechanism of electrochemical reduction of oxygen under certain conditions, the analysis gives no information about the microscopic details

Table 1 Reaction mechanism for oxygen reduction on an LSM electrode and the corresponding charge transfer coefficients [5]

Step	Reaction	α_a	α_c
1	$O_2(g) \rightarrow 2O_{ad}$	—	—
2	$O_{ad} + e^- \rightarrow O_{ad}^-$	3/2	1/2
3	$O_{ad}^- \rightarrow O_{TPB}$	1	1
4	$O_{TPB}^- + e^- + V_O^{\bullet\bullet} \rightarrow O_O^{\times}$	—	—

of the reaction. The characteristics of oxygen reduction at a Pt/YSZ interface [12] were reported to be similar to those at an LSM/YSZ interface [11]. However, oxygen reduction can take place only at the TPB for a Pt electrode, while both the TPB and the surface of the LSM can be active in principle, especially when the cathodic overpotential is relatively high. Therefore, more information is needed to understand the oxygen reduction on an LSM electrode.

In this paper, we report the observed electrochemical behavior of $La_{0.9}Sr_{0.1}MnO_3$ -based electrodes supported on a YSZ or a LSGM electrolyte as studied using DC polarization, impedance spectroscopy, and a potential step method, in an effort to elucidate the electrode kinetics and reaction mechanism of oxygen reduction on an LSM electrode.

Experimental

YSZ electrolyte pellets were prepared from a commercial YSZ powder (8 mol% Y_2O_3 -doped ZrO_2 , Tosoh) by pressing at 6000 psi for 1 min followed by sintering at 1773 K for 6 h. The thicknesses of the YSZ pellets were about 1 mm and the diameters were about 16 mm.

La_2O_3 , $SrCO_3$, Ga_2O_3 , and MgO were used as precursors for the preparation of the $La_{0.9}Sr_{0.1}Ga_{0.9}Mg_{0.1}O_3$ (LSGM) electrolyte [13]. Powders with stoichiometric compositions were ball-milled in ethanol for 24 h and calcined at 1373 K for 5 h to form the perovskite phase. X-ray powder diffraction (Philips, PW 1800) was used to determine the phase composition of the calcined products. Powders with the perovskite phase were crushed using an agate mortar-and-pestle and then ball-milled in ethanol for 24 h. The resulting fine powders were pressed into pellets (with a diameter of 20 mm and thickness of 1 mm) at 6000 psi for 1 min and sintered at 1773 K for 6 h.

$La_{0.9}Sr_{0.1}MnO_3$ (LSM) perovskite powder was synthesized using the Pechini method, starting from the precursors La_2O_3 , $SrCO_3$, and $MnCO_3$. The phase composition of the prepared LSM was confirmed using X-ray diffraction. LSM-YSZ and LSM-LSGM composite electrodes were prepared by thorough mixing and grinding the LSM powder with 20 wt% corresponding electrolyte powders.

A three-electrode assembly was used to investigate the electrochemical properties of the electrodes, as shown in Fig. 1 [6, 8, 11]. LSM paste, which was prepared through mixing the LSM powder with an appropriate amount of organic binder and solvent, was painted on one side of the electrolyte as a working electrode. The electrode/electrolyte assemblies prepared included LSM/YSZ, LSM-YSZ/YSZ, LSM-LSGM/YSZ, LSM/LSGM, LSM-YSZ/LSGM, and LSM-LSGM/LSGM. The area of each electrode was about 0.3 cm^2 and the thickness was about $10 \mu\text{m}$. The working electrodes were fired at 1473 K in air for 2 h before the application of counter and reference electrodes.

Pt counter and reference electrode were prepared by screen-printing Pt paste (Engelhard) on the other side of the electrolyte, followed by sintering at 1123 K for 2 h. The areas of the Pt counter and reference electrodes were about 0.8 and 0.1 cm^2 , respectively.

The electrode/electrolyte assembly was placed in an appropriately designed quartz reactor and exposed to flowing air. Pt grids were attached and pressed with springs on the working and counter electrodes as current collectors. Three Pt wires were connected to the working, counter, and reference electrodes and led to a potentiostat/galvanostat. The flow rate of air was about 100 mL min^{-1} .

All electrochemical measurements were carried out with an EG&G 273A potentiostat/galvanostat and a 5201 lock-in amplifier. The frequency range of impedance measurements was from

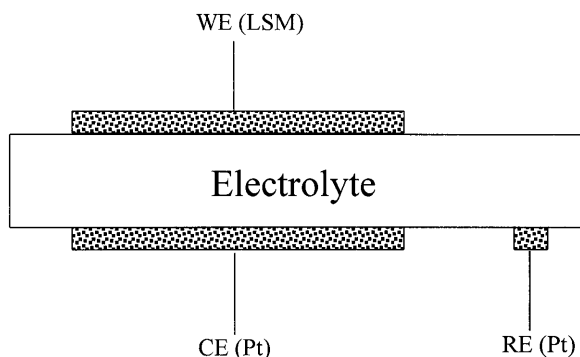
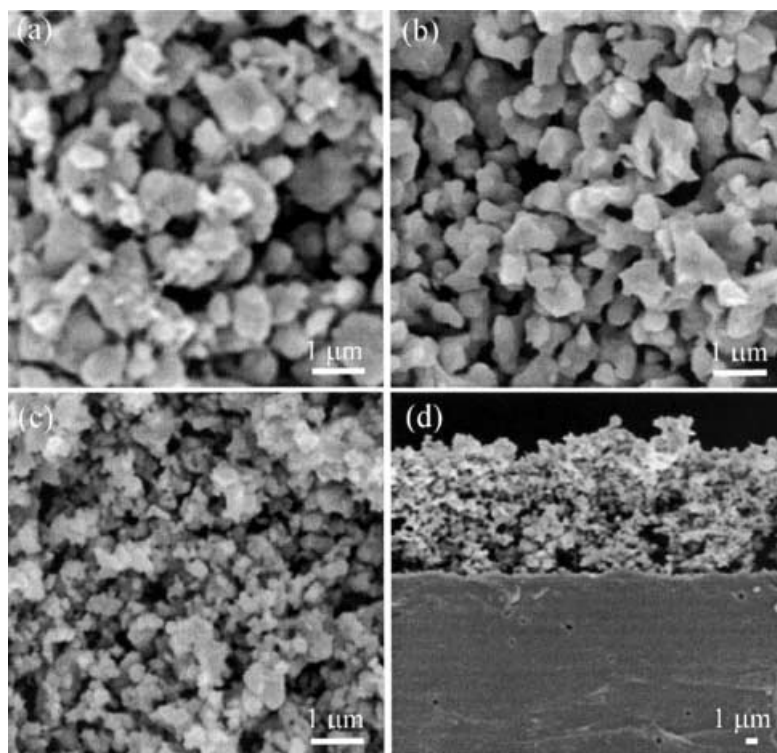


Fig. 1 A schematic diagram showing the three-electrode configuration used for electrochemical testing (WE=working electrode, CE=counter electrode, RE=reference electrode)

0.01 Hz to 100 kHz, and the amplitude of the applied AC voltage was 5 mV. The spectra were recorded at 5 points per decade. Ohmic resistance of the electrolyte and Pt wire was determined from the impedance at the high-frequency limit ($\omega \rightarrow \infty$) [6].

A potential step method was used to study the time dependence of the interfacial properties during polarization. Recently, it has been used to characterize the formation and spillover of oxygen vacancies over LSM electrodes [6, 8]. In a typical potential step experiment, the working electrode was first subjected to a -0.8 V potential with respect to the reference electrode until the current reached a stable value. Then, the potential applied to the electrode was stepped to 0.4 V to eliminate the oxygen vacancies in the electrode. After the anodic current reached a steady-state value, the potential applied to the working electrode was then stepped back to -0.8 V and the current response was recorded as a function of time. The microstructures of the samples after electrochemical testing were examined using a scanning electron microscope (SEM, Hitachi S-800).

Fig. 2 SEM micrographs of the top views of **a** LSM, **b** LSM-YSZ, and **c** LSM-LSGM electrodes, and **d** the cross-sectional view of an LSM-YSZ/YSZ interface. All of the electrodes were fired at 1473 K for 2 h



Results and discussion

Microstructure

Shown in Fig. 2 are some typical surface microstructures of the three LSM-based electrodes. The average grain sizes of the electrodes vary from $0.15 \mu\text{m}$ for LSM-LSGM, to $0.5 \mu\text{m}$ for LSM-YSZ, and to $1 \mu\text{m}$ for LSM. Clearly, the addition of electrolyte powder into LSM hinders the grain growth of LSM particles during firing, thus increasing the surface area for electrode reaction. The cross-sectional view of an LSM-LSGM/YSZ interface, shown in Fig. 2d, indicates that the adhesion of the electrode to the electrolyte appears to be sufficient and the thickness of the electrode is about $10 \mu\text{m}$.

Impedance spectroscopy and polarization near equilibrium

Shown in Fig. 3 are some typical impedance spectra of LSM/LSGM and LSM/YSZ interfaces. The interfacial resistances (R_p), as determined from the impedance spectra shown in Fig. 3, are similar to those determined from linear polarization measurements. Shown in Fig. 4 are plots of T/R_p versus $1/T$ for the different electrodes studied. Clearly, the interfacial resistances of the pure LSM and LSM-YSZ electrodes supported on a YSZ electrolyte are far smaller than those supported on an LSGM electrolyte, implying that the oxygen reduction

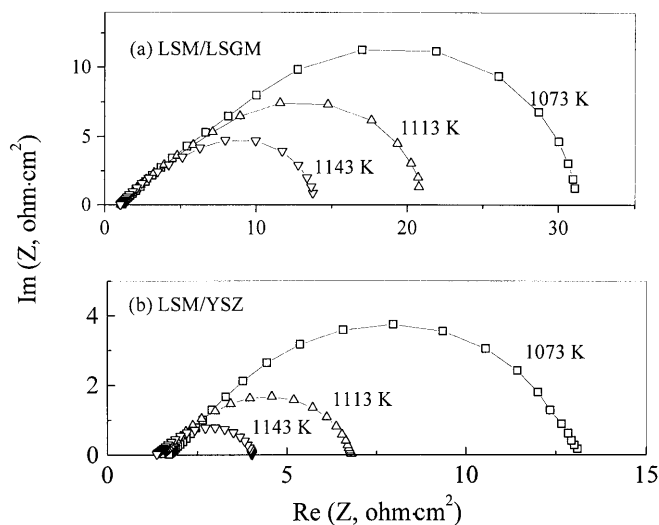


Fig. 3 Impedance spectra of **a** LSM/LSGM and **b** LSM/YSZ interfaces in air under open circuit conditions. The number adjacent to each line represents the temperature at which the impedance spectra were acquired

on LSM electrodes depends strongly on the properties of the TPB (which involves the electrolyte), although the surface of the LSM could be active since LSM is still a mixed conductor.

Listed in Table 2 are the activation energies of T/R_p as calculated from the Arrhenius plots shown in Fig. 4. The activation energies for oxygen reduction on LSM-YSZ and LSM-LSGM composite electrodes varied from 130 to 170 kJ mol^{-1} , but showed little dependence on the nature of the electrolyte used. However, the activation energy for oxygen reduction on a pure LSM electrode was strongly affected by the nature of the electrolyte, varying from 230 kJ mol^{-1} for an LSM/YSZ interface to about 120 kJ mol^{-1} for an LSM/LSGM interface. The exchange current densities of LSM-based electrodes supported on YSZ were much higher than those supported on LSGM, as shown in Table 2, except for the LSM-LSGM electrode, further confirming that the electrode kinetics on an LSM electrode depends strongly on the properties of the TPB. The observed high catalytic activity of LSM-LSGM/LSGM is due probably to the existence of more TPB as well as the good compatibility between the LSM-LSGM electrode and the LSGM electrolyte. It is noted, however, that the LSM/YSZ interface is different from the LSM-YSZ/YSZ interface and the properties of the composite LSM electrodes depend on the composition and the subsequent processing conditions.

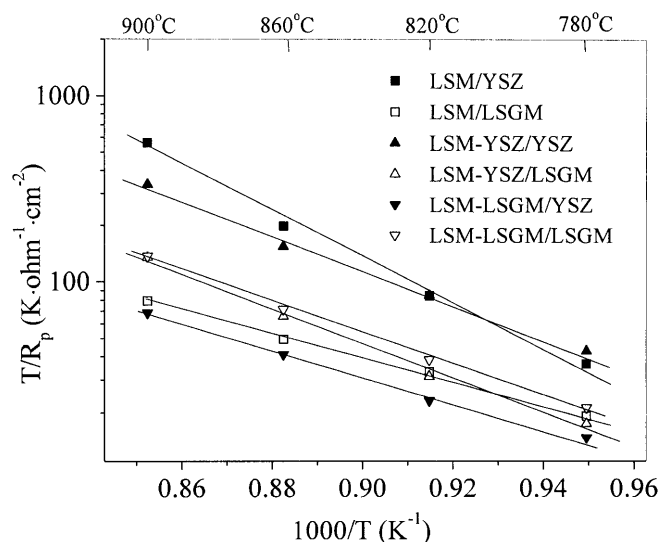


Fig. 4 Arrhenius plots for various LSM-based electrodes supported by either YSZ or LSGM. The slopes of these plots are related to the activation energies for the interfacial processes, as tabulated in Table 2

Impedance spectroscopy and polarization far away from equilibrium

Shown in Fig. 5 are some typical impedance spectra of a pure LSM electrode supported on LSGM and YSZ under high overpotential polarization. Most of the impedance spectra could be deconvoluted into two arcs. In general, the impedance decreased considerably with the value of the applied DC cathodic overpotential, implying that the charge transfer processes are dominating the overall process. The polarization resistances calculated from impedance spectra were close to those calculated from DC polarization for the LSM/YSZ interfaces. However, the interfacial resistances of LSM/LSGM determined from impedance spectra were smaller than those determined from DC polarization. The discrepancy between the impedance data and the DC polarization data is due probably to the relaxation properties of the LSM/LSGM interface, as explained below [5].

The size of the arc at high frequencies showed little dependence on the value of the applied DC overpotential; however, the size of the arc at low frequencies decreased with the value of the applied DC overpotential, implying that the low-frequency arc was closely related to charge transfer steps. The impedance spectra were dominated by the low-frequency arc, i.e., charge transfer process, especially under relatively low overpotentials.

Table 2 Activation energies of T/R_p and exchange current densities (at 1173 K) of LSM-based electrodes

	LSM/YSZ	LSM/LSGM	LSM-YSZ/YSZ	LSM-YSZ/LSGM	LSM-LSGM/YSZ	LSM-LSGM/LSGM
E_a (kJ mol^{-1})	2.3×10^2	1.2×10^2	1.7×10^2	1.7×10^2	1.3×10^2	1.5×10^2
i_0 (mA cm^{-2})	24	3.4	15	5.8	2.9	5.9

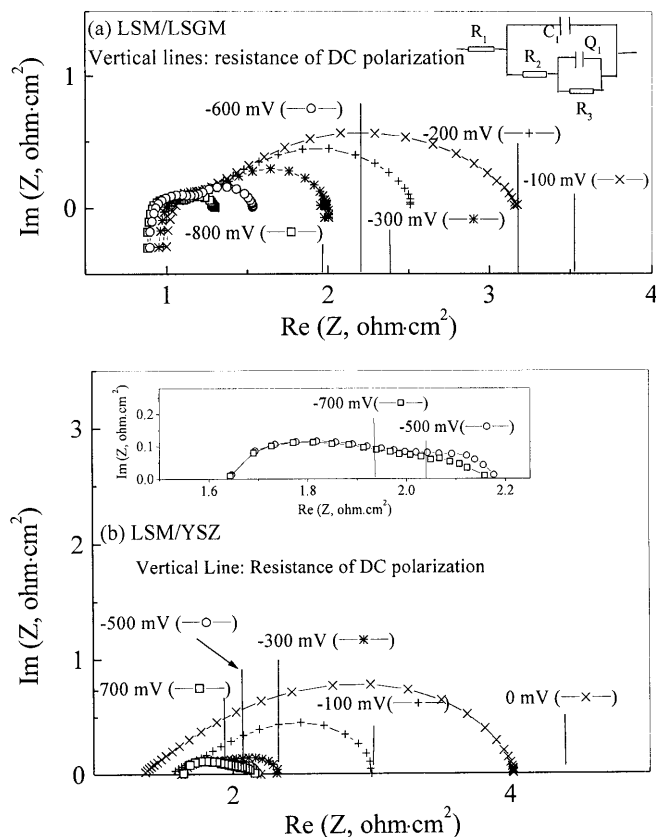


Fig. 5 Impedance spectra of **a** LSM/LSGM and **b** LSM/YSZ electrodes as measured in a three-electrode configuration under various cathodic polarizations at 1173 K. The number adjacent to each spectrum represents the value of the DC polarization applied to the cell while the impedance was acquired

Shown in Fig. 6 are the results of DC polarization at the LSM/YSZ and LSM/LSGM interfaces at different temperatures. All DC polarization experiments were recorded when a steady state was reached, and the time required to reach an equilibrium state for each DC polarization measurement varied with the experimental conditions. It can be seen that the current passing through an LSM/LSGM interface is far lower than that through an LSM/YSZ interface. In either case, however, a Tafel region is apparent at high overpotentials. Listed in Table 3 are the cathodic charge transfer coefficients and exchange current densities of the two electrodes as determined from the data shown in Fig. 6. The exchange current densities of the two electrodes are similar, especially at high temperatures. The cathodic charge

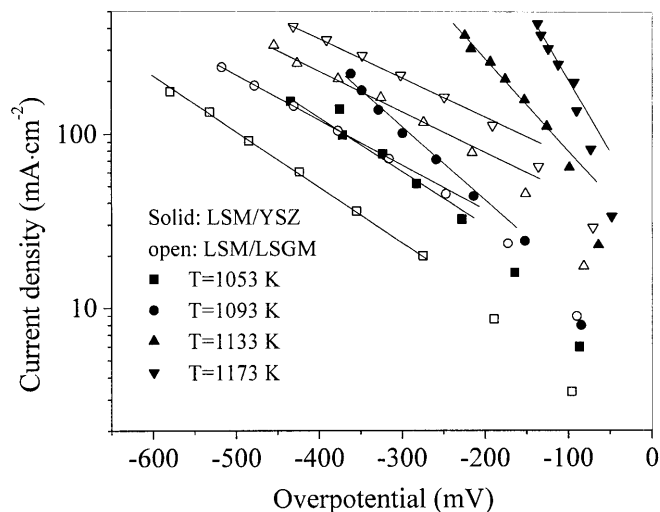


Fig. 6 Cathodic polarization of an LSM electrode supported on YSZ and LSGM at various temperatures

transfer coefficient of oxygen reduction at an LSM/LSGM interface was about 0.5, and that at an LSM/YSZ interface was about 1 at high temperatures (1093–1133 K). The variation of α_c could be caused by a change in r.d.s. with operating temperature. As can be seen from the impedance spectra, there are two arcs in each spectrum and the size of them changed with temperature and with the value of the overpotential applied to the electrode. The calculation of α_c is based on the assumption that the overall reaction is dominated by one r.d.s., i.e., the low-frequency arc in this experiment; however, the high-frequency arc was comparable with the low-frequency arc under high overpotentials. Therefore, the value of α_c could be affected by the high-frequency arc under high overpotentials. Theoretically, the resistance corresponding to each arc can be calculated from the impedance spectrum. Since we are primarily interested in the general effect of electrolytes on the performance of an LSM electrode, we used the DC polarization data to approximate the value of α_c . However, it is noted that the exchange current densities determined from linear polarization (Table 2) are smaller than those determined from Tafel polarization (Table 3). This is due primarily to the change in catalytic and transport properties of the LSM under the influence of a large-value DC polarization, as explained in detail in the next section.

Table 3 Charge transfer coefficients and exchange current densities for oxygen reduction on an LSM electrode supported on YSZ and LSGM electrolytes

	1053 K		1093 K		1133 K		1173 K	
	α_c	i_0 (mA cm ⁻²)	α_c	i_0 (mA cm ⁻²)	α_c	i_0 (mA cm ⁻²)	α_c	i_0 (mA cm ⁻²)
LSGM/LSM	0.6	3.9	0.6	11	0.5	28	0.5	49
YSZ/LSM	0.6	10	1.0	13	1.1	26	1.4	53

Shown in Fig. 7 are the polarization curves of different electrodes as measured at 1173 K. It can be seen that, for a given cathodic polarization, the electrodes supported on YSZ exhibit higher catalytic activity than those supported on LSGM, consistent with results of linear polarization. Further, the calculated cathodic charge transfer coefficient, α_c , is about 1 for the LSM/YSZ interface and about 0.5 for the LSM/LSGM interface at high temperatures. According to the model in Table 1, it is most likely that the r.d.s. of oxygen reduction on an LSM electrode supported on YSZ is the diffusion of partially reduced oxygen species from the electrode surface to the TPB, while that on LSGM is electron donation to adsorbed oxygen atoms.

Current relaxation measurements

Shown in Fig. 8 are some typical current relaxation curves when the working electrode (LSM) was stepped to a potential of -0.8 V with respect to a Pt reference electrode. The two cells based on different electrolytes, LSM/YSZ/Pt and LSM/LSGM/Pt, showed very different behavior. The current passing through LSM/YSZ/Pt increased with time whereas that passing through LSM/LSGM/Pt decreased with time, implying that the current relaxation is dominated by the TPB, not by the LSM/gas interface.

Previous studies [5, 8, 14] suggested that the increase of cathodic current through an LSM/YSZ interface could be related to the increase of mixed conductivity in LSM electrodes as a consequence of Mn^{3+} reduction and oxygen vacancies formation, which extends the active area from the TPB to the surface of the LSM electrode. The spillover of oxygen vacancies on an LSM electrode, supported on YSZ, was recently verified by Horita et al. [15], using SIMS under certain conditions. However, the extension of the active region for oxygen

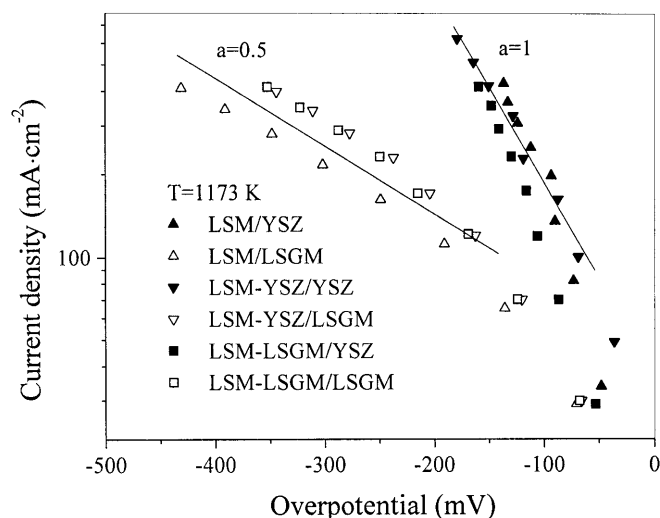


Fig. 7 Polarization curves of various samples at 1173 K

reduction is unlikely for an LSM supported on LSGM since the cathodic current decreases with time.

The dramatic difference between the cathodic charge transfer coefficients for oxygen reduction at the LSM/YSZ and LSM/LSGM interfaces also suggests that the oxygen reduction at the LSM/LSGM interface is primarily limited by the TPB reaction and the LSM/gas interface reaction does not contribute significantly to the overall electrode reaction. If the LSM/gas interface indeed contributes significantly to the overall electrode reaction for both the LSM/YSZ and the LSM/LSGM interfaces, the oxygen reduction at the two interfaces should exhibit similar characteristics.

The strong dependence of current relaxation on electrolytes is likely to be related to the dependence of reaction kinetics on the electrode/electrolyte interface. The oxygen reduction at an LSM/LSGM interface is limited to the TPB at the moment when a cathodic

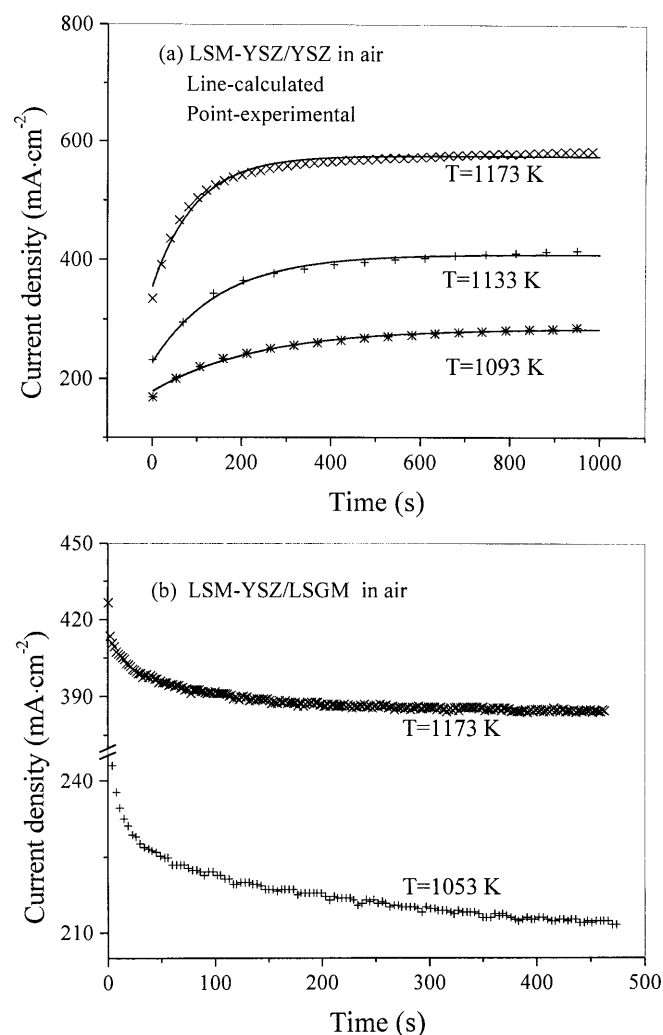


Fig. 8 Current relaxation of a LSM-YSZ/YSZ and b LSM-YSZ/LSGM after the potential of the working electrode was stepped at -0.8 V at different temperatures. The temperature adjacent to each curve represents the temperature at which the experiment was performed

potential is applied to the interface, considering that LSM is a poor mixed conductor [16]. Since the oxygen reduction at an LSM/LSGM interface is controlled by the electron donation to oxygen atoms, the extra oxygen atoms at the interface and the surface of LSM electrode could limit the formation and spillover of oxygen vacancies on the surface of the LSM electrode. As for the LSM/YSZ interface, the reaction is controlled by the diffusion of the partially reduced oxygen species, and the active region is not limited only to the TPB. The increase in concentration of oxygen vacancies will improve the diffusion of "charged species", leading to a significant increase of catalytic activity.

The inter-diffusion of elements between LSM and LSGM might take place at high temperatures. However, a recent study [17] indicated that the inter-diffusion/reaction between LSM and LSGM is insignificant at 1743 K for 10 h. Thus, it seems that the kinetics of oxygen reduction at an LSM/electrolyte interface and its relaxation characteristics are determined primarily by the behavior of the TPB.

Conclusions

The kinetics of oxygen reduction at an LSM/electrolyte interface shows strong dependence on the nature of the electrolyte. The cathodic charge transfer coefficient is about 1 at an LSM/YSZ interface at high temperatures, implying that the r.d.s. is the diffusion of partially reduced oxygen species, and about 0.5 for an LSM/LSGM interface, indicating that the r.d.s. is the donation of electrons to atomic oxygen. The impedance of both interfaces decreases with the value of the applied DC cathodic overpotential, because the charge transfer, rather than the mass transfer, is dominating the electrode kinetics. LSM electrodes supported on YSZ exhibit a higher catalytic activity than those supported on LSGM.

The relaxation properties of the LSM electrodes show an even more dramatic dependence on the nature of the electrolyte. Under cathodic polarization, the current increases for an LSM/YSZ interface, but decreases for an LSM/LSGM interface, further confirming that the oxygen reduction at an LSM/electrolyte interface depends strongly on the electrolyte.

Acknowledgements This work was supported by the NSF under grant nos. CTS-9705541 and CTS-9819850.

References

1. Ishihara T, Honda M, Shibayama T, Minami H, Nishiguchi H, Takita Y (1998) *J Electrochem Soc* 145:3177
2. Ishihara T, Matsuda H, Takita Y (1994) *J Am Chem Soc* 116:3801
3. Huang PN, Petric A (1996) *J Electrochem Soc* 143:1644
4. Baker RT, Gharbage B, Marques FMB (1997) *J Electrochem Soc* 144:3130
5. van Heuveln FH, Bouwmeester HHM (1997) *J Electrochem Soc* 144:134
6. Wang S, Jiang Y, Zhang Y, Yan J, Li W (1998) *J Electrochem Soc* 145:1932
7. Siebert E, Hammouche A, Kleitz M (1995) *Electrochim Acta* 40:1741
8. Jiang Y, Wang S, Zhang Y, Yan J, Li W (1998) *J Electrochem Soc* 145:373
9. Gharbage B, Pagnier T, Hammou A (1994) *J Electrochem Soc* 141:2118
10. Bockris JO'M, Reddy AKN (1977) *Modern electrochemistry*, vol 2. Plenum Press, New York
11. Jiang Y, Wang S, Zhang Y, Yan J, Li W (1998) *Solid State Ionics* 110:111
12. Wang DY, Nowick AS (1979) *J Electrochem Soc* 126:1155
13. Chen F, Liu M (1998) *J Solid State Electrochem* 3:7
14. Lee HY, Cho WS, Oh SM, Wiemhöfer H-D, Göpel W (1995) *J Electrochem Soc* 142:2659
15. Horita T, Yamaji K, Sakai N, Yokokawa H, Kawada T, Kato T (2000) *Solid State Ionics* 127:55
16. Liu M (1998) *J Electrochem Soc* 145:142
17. Huang K, Feng M, Goodenough JB, Schmerling M (1996) *J Electrochem Soc* 143:3630